VILNIUS UNIVERSITY
CENTER FOR PHYSICAL SCIENCES AND TECHNOLOGY

Domas
BALČIŪNAS

Synthesis and Investigation of Glyphosate Sensitive Molecular Imprints in a Polypyrrole Matrix

SUMMARY OF DOCTORAL DISSERTATION

Natural science,
Chemistry (N 003)

VILNIUS 2021

This dissertation was written between 2016 and 2021 at Vilnius University, Faculty of Chemistry and Geosciences.

Academic supervisor:

Doc. dr. Deivis Plausinaitis (Vilnius University, Natural Sciences, chemistry – N 003).

Academic consultant:

Prof. habil. dr. Arunas Ramanavicius (Vilnius University, Natural Sciences, chemistry – N 003).

This doctoral dissertation will be defended in a public meeting of the Dissertation Defence Panel:

Chairman – **Prof. habil. dr. Rimantas, Ramanauskas** (Center for Physical Sciences and Technology, Natural sciences, Chemistry – N 003).
Members:
Doc. dr. Virgaudas Kubilius (Vilnius University, Natural sciences, Chemistry - N 003).
Doc. dr. Aušra Valiūnienė (Vilnius University, Natural sciences, Chemistry - N 003).
Prof. dr. Vida Vičkačkaitė (Vilnius University, Natural sciences, Chemistry - N 003).
Dr. Roman Viter (University of Latvia, Natural sciences, Chemistry – N 003).

The dissertation shall be defended at a public meeting of the Dissertation Defence Panel at 12:00 (hour) on 29th of October 2021 in TChA lecture hall of the Faculty of Chemistry and Geoscience Chemistry Institute (Vilnius University).
Address: Naugarduko street 24, LT-03225, Vilnius, Lithuania. Tel.: 8 (5) 219 3105, e-mail: info@chgf.vu.lt.
The text of this dissertation can be accessed at the libraries of (name of the institutions granted the right to conduct doctoral studies in alphabetical order), as well as on the website of Vilnius University: www.vu.lt/lt/naujienos/ivykiu-kalendorius

VILNIAUS UNIVERSITETAS
FIZINIŲ IR TECHNOLOGIJOS MOKSLŲ CENTRAS

Domas
BALČIŪNAS

Glifosatui jautraus molekulinių įspaudų polipirolo matricoje jutiklio sintezė ir tyrimas

DAKTARO DISERTACIJOS SANTRAUKA

Gamtos mokslai,
Chemija (N 003)

Disertacija rengta 2016 – 2021 metais Vilniaus Universitete, chemijos ir geomokslų fakultete.

Mokslinis vadovas:

Doc. dr. Deivis Plaušinaitis (Vilniaus universitetas, gamtos mokslų sritis, chemija – N 003).

Mokslinis konsultantas:

Prof. habil. dr. Arūnas Ramanavičius (Vilniaus universitetas, gamtos mokslų sritis, chemija – N 003).

Gynimo taryba:

Pirmininkas – **Prof. habil. dr. Rimantas Ramanauskas** (Fizinių ir technologijos mokslų centras, gamtos mokslai, chemija – N 003).

Nariai:
Doc. dr. Virgaudas Kubilius (Vilniaus universitetas, gamtos mokslai, chemija– N 003).
Doc. dr. Aušra Valiūnienė (Vilniaus universitetas, gamtos mokslai, chemija– N 003).
Prof. dr. Vida Vičkačkaitė (Vilniaus universitetas, gamtos mokslai, chemija– N 003).
Dr. Roman Viter (Latvijos universitetas, gamtos mokslai, chemija – N 003).

Disertacija ginama viešame gynimo tarybos posėdyje 2021 m. Spalio mėn. 29 d. 12:00 val. Vilniaus universiteto chemijos ir geomokslų fakulteto chemijos instituto Taikomosios chemijos (TChA) auditorijoje. Adresas: Naugarduko g. 24, LT-03225 Vilnius, Lietuva. Tel.: 8 (5) 219 3105, el. paštas: info@chgf.vu.lt.

Disertaciją galima peržiūrėti Vilniaus universiteto ir FTMC bibliotekose bei VU interneto svetainėje adresu: *https://www.vu.lt/naujienos/ivykiu-kalendorius*

TABLE OF CONTENT

INTRODUCTION

The class of electrochemically synthesized electrically conductive polymers (CP), such as one of them, polypyrrole (Ppy), has been of great interest to scientists for more than 30 years. The use of such materials is very widespread: they are used as elastic textile composites with high electrical conductivity, in the production of ion exchange membranes, secondary batteries or supercapacitors, also in graphite fibres in order to increase resistance to shear deformation and strength, etc.

The ability of polypyrrole to change between oxidized and reduced states allows this material to become conductive or insulating, which is also of considerable interest. However, in this work we aim to synthesize conductive layers of polypyrrole that would allow us to more easily study the analytical properties of this polymer as a sensitive material. Another advantage of such a polymer is biocompatibility. Ppy is an effective immobilizing agent that can be easily obtained by both chemical and electrochemical polymerization. Electropolymerization is a simple and clear method of precipitating polymer coatings, the use of which is still growing in the development of bio- and immunosensors.

Artificial receptors are becoming an increasingly important alternative to immobilized molecules in analytical systems. These receptors leave an artificial molecular imprint in its matrix which is then able to recognize only the specific molecule under study. The basis of such artificial receptors is electrically conductive polymers, which is why this technology has been named as molecularly imprinted polymers (MIP) technology.

The active ingredient in all the world's most widely used herbicides is glyphosate (Gly). There is currently a lot of debate about the use of glyphosate, but medical researchers agree that glyphosate can cause cancer, respiratory diseases (asthma), neurological diseases (Parkinson's disease), congenital disorders (congenital or fertility-related effects) or other diseases such as kidney disorder,

gastroschisis, etc. The growing use of herbicides in agriculture is also significantly increasing the need to develop a sensitive, selective and reliable research method of this component. MIP technology could be a great choice for glyphosate sensor development.

The research done in this study describes the electrosynthesis tendencies of electrically conductive polypyrrole layer which was synthesized by multicycle double step potential chronoamperometry (McDsP) method. Also shows the properties and limitations of coatings such as a potential MIP sensor for a glyphosate molecule. Coatings were formed on both bare and self-assembled monolayer modified gold electrode surfaces. Surface studies were performed by electrochemical impedance spectroscopy (EIS), cyclic voltammetry (CV), chronoamperometry and surface plasmon resonance (SPR) methods.

The aim of this research:

To study the tendencies of formation of electrically conductive polymer polypyrrole layer on gold surface and to find the most suitable electropolymerization conditions for MIP sensor electrosynthesis.

To form MIP coatings on pure gold surface and on gold modified self-assembled monolayer (SAM) and to perform glyphosate adsorption / desorption experiment on formed systems using combined electrochemical measurements with surface plasmon resonance (ESPR) technology.

The objectives of this research:

1. To form electrically conductive polymer Ppy layers on a gold electrode surface in acetonitrile solution by using different pyrrole concentrations in a polymerization solution and by performing electropolymerization with a different number of McDsP pulses.

2. To study the electrical properties of Ppy layers on gold surface obtained by different monomer solution concentrations and different number of pulses by McDsP method.
3. Evaluate the results obtained from the layers forming experiments and select the most suitable polymerization conditions for the MIP sensor electrosynthesis.
4. To form four systems on the gold surface under selected electropolymerization conditions: Ppy on gold (NIPpy); MIP on gold (MIPpy); Ppy on SAM deposited on gold (SAM / NIPpy); MIP on SAM deposited on gold (SAM / MIPpy). Perform all synthesis in an ESPR cell.
5. Investigate the process of formation and features of formed systems using the ESPR research method.
6. To perform adsorption / desorption studies of the most common herbicide active substance glyphosate on formed systems by ESPR method.

The statements to defend:

1. Prior to oxidation of the pyrrole, a certain monomer ad-layer is formed on the surface of the gold electrode in the polymerization solution.
2. While forming Ppy layer by McDsP method, applying further pulses results to increase of electrically conductive polymer area in a solution-ppy phase contact boundary. However, a layer-by-layer polymer structure is possible later on, so that the gold surface can be completely electrically blocked by a low-conductive polypyrrole.
3. During MIPpy electrosynthesis, the presence of glyphosate molecules in a polymerization solution influences the current flowing rate and the formation of a layer during an oxidation pulse.

4. MIPpy layers on the Au electrode surface can be used for the development of a glyphosate-sensitive sensor.

1. METHODS AND MATERIALS

1.1 Reagents

For the preparation of AcN medium solutions (AcN-TBAPF$_6$) we used high performance liquid chromatography grade acetonitrile (99.95%) from ROTH (CAS: 75-05-8) and tetrabutylammonium hexafluorophosphate (TBAPF$_6$) salt from Alfa Aesar (CAS: 3109-63-5).

Aqueous PBS solutions were prepared from freshly distilled first purity class water (0.055 μS/cm at 25 °C), 10 mM NaH$_2$PO$_4$·2H$_2$O (99%) from Eurochemicals (CAS: 7558-80-7), 50 mM Na$_2$HPO$_4$·12H$_2$O (98%) from Eurochemicals (CAS: 7558-79-4) and 50 mM Na$_2$SO$_4$·10H$_2$O (99%) from Sigma-Aldrich (CAS: 7727-73-3) and adjusted with H$_2$SO$_4$ (96%) from Eurochemicals (CAS: 7664-93-9) until an accurate pH of 7.0 was reached.

For the preparation of polymerization solutions we used 98% pyrrole from AlfaAesar (CAS: 109-97-7) which was further purified by passing the solution through 5 cm long column of Al$_2$O$_3$. For MIP polymerization solutions preparation we used a 360 g/l aqueous glyphosate solution from ADAMA Agan LTD (CAS: 38641-94-0).

11-(1H-pyrrol-1-yl)-undecan-1-thiol (PUT) (96%) from Sigma-Aldrich (CAS: 141779-05-7) and 96% ethanol (EtOH) from Vilnius Degtinė (CAS: 200-578-9) were used to deposit SAM on the surface of gold electrode.

We used 0.1 M HCl (35-38%) from Avsista (CAS: 231-595-7) to clean the surface of the SPR gold chip, and the surface of the Gamry electrode was polished with Al$_2$O$_3$ powder.

1.2 Prepared solutions

AcN-TBAPF$_6$ solutions were prepared from 0.01 M TBAPF$_6$ and 5% (v /v) water in AcN solution. For preparation of AcN-TBAPF$_6$-Py we added pyrrole to the polymerization solution respectively 5; 10; 25 and 50 mM, which will be indicated in this work as C$_{Py}$ = 5; 10, 25; 50 mM.

Aqueous PBS solutions were prepared from 10 mM NaH$_2$PO$_4$·2H$_2$O, 50 mM Na$_2$HPO$_4$·12H$_2$O and 50 mM of Na$_2$SO$_4$·10H$_2$O was added to improve ionic conductivity. H$_2$SO$_4$ was also added dropwise until a pH of 7.0 was reached. To the polymerization solution PBS$_{Py}$, 50 mM of pyrrole was additionally added. And to the MIP polymerization solution PBS$_{Py+Gly}$ 5 mM of glyphosate was mixed. True, both PBS$_{Py}$ and PBS$_{Py+Gly}$ were diluted 5-fold after injection into the SPR cell, so we had C$_{Py}$ = 10 mM and C$_{Gly}$ = 1 mM in the final polymerization solutions.

For glyphosate adsorption / desorption studies of the formed MIP and NIP layers, we used PBS$_{Gly}$ solutions, which were prepared by adding various concentrations of Gly (C$_{Gly}$ = 0.25 mM; 0.5 mM; 1 mM; 2 mM; 2.5 mM) in PBS.

The SAM precipitation solution was prepared by adding 1 mM PUT to EtOH, which also finally diluted 5-fold.

0.1 mM HCl solution was prepared to clean the SPR sensor chip.

1.3 Instrumentation

For the experiments performed in AcN medium, we used a three-electrode branded Dr. Bob Gamry's cell. The cell had a three-electrode system consisting of: (i) a working gold electrode with a working diameter of 3 mm and a geometric surface area of 0.07 cm^2, (ii) a reference Ag/AgCl/NaCl (saturated) electrode and (iii) a platinum wire auxiliary electrode.

CV, EIS, and chronoamperometry experiments were performed using a "Reference 600" potentiostat controlled by the Gamry Instruments Framework (version 5.30) software, both from Gamry (Warminster Township, United States).

For ESPR measurements, we used "Autolab ESPRIT" from Eco Chemie BV (Netherlands). The device has a built-in electrochemical cell that also uses a 3-electrode system. The equipment was managed by "Data Acquisition" software (version 4.5) from Methrom Autolab B.V. (Netherlands). Kinetic Evaluation software (version 5.4), also from Methrom Autolab B.V., was used to process the data received.

The SPR gold chip was prepared by using "PVD 75" from the Kurt J. Lesker Company (USA) magnetron sputter deposition system. A 25 mm diameter 1 mm thick disc-shaped glass chip was coated with a layer of titanium or chromium ~1 nm thick and ~50 nm thick gold coating [1].

During the ESPR experiments, we controlled the SPR cell temperature at 298.0 ± 0.5 K by using a "UTU-4 ultrathermostat" (Poland) thermostat.

1.4 The course of experiments

1.4.1. Electrosynthesis of Ppy layer in AcN medium by McDsP method

First, the Gamry working electrode was polished in 0.3 μm alumina powder and then kept in an ultrasonic bath for 5-10 min. After that the electrode was prepared electrochemically, 3 CV cycles were spread in the range of -0.5...+ 2.0 V. From the curves recorded during the CV experiment, following the methodology used in other publications [2], we calculated the electric charge passed during oxygen desorption process, which was equal to 105 μC. Knowing that the oxygen desorption flux at the Au surface is 390 $\mu C/cm^2$, we determined that the electrode roughness factor is 3.85.

For evaluation of electrode surface preparation, EIS spectra were recorded in the same solution after each cleaning procedure. After

evaluating that the surface cleaning was successful, we changed the AcN-TBAPF$_6$ solution to the AcN-TBAPF$_6$-Py polymerization solution and started the electropolymerization process.

One of the aims of the experiments was to evaluate the dynamics of Ppy formation on the Au electrode surface in AcN-TBAPF$_6$ solution during electrochemical polymerization using different concentrations of pyrrole in the polymerization solution. Therefore, all Ppy formation experiments were performed by McDsP method: sequence of 1, 5, 10 or 20 potential pulses at 0.0 and 1.0 V vs Ag / AgCl was maintained for 10 sec.

After Ppy layer deposition EIS spectrum was registered.

1.4.2. Synthesis and investigation of glyphosate sensitive MIP by ESPR method

In particular, the surface of the working electrode was also cleaned both chemically and electrochemically, thus preparing it for experiments. Initially, throughout the system for 150 sec. distilled water was pumped, then it was changed to 0.1 M HCl solution. This solution was pumped for another 200 sec, then it was returned to the dist. H$_2$O and pumped through the system for another 200 sec. Finally, the cell was filled with PBS solution, and convincing that the SPR difference curve is close to 0 m°, we cleaned the electrode by CV method, spreading two potential cycles in the range of -0.4 ... + 1.0 V.

Also, from the obtained cyclic voltammerograms, using the methodology mentioned above [2], we calculated the electric charge flow rate during oxygen desorption also, which was equal to 40 μC, and from this we determined the electrode roughness factor - 1.30. Again, EIS spectra were recorded for evaluation of electrode preparation after surface preparation.

The polymerization solution (PBS$_{Py}$ to form NIPpy or PBS$_{Py+Gly}$ to form MIPpy) was then injected into the measuring cell using a semi-automated sample injector. Electropolymerization of the NIPpy and MIPpy layers was performed by applying a single

chronoamperometric pulse (step from 0 to 1 V maintained for 7 sec. *vs* Ag/AgCl electrode). After formation, the layer was washed with pure PBS (without Gly and without Py) solution by pumping it through an electrochemical cell at 80 μl/sec. velocity. The glyphosate adsorption experiment was then started by adding 20 μl of 1 mM PBS_{Gly} solution. The change of SPR signal over time was monitored and recorded. Next, SPR cell was washed again with PBS and the SPR signal was monitored for its ability to return to previous values. EIS spectra were also recorded before and after each experimental step.

The association of glyphosate on the Au surface was evaluated by CV experiment, the potential in PBS_{Gly} solution was spread in the range of -0.40...+ 1.25 V, scanning speed 50 mV/s, potential step 3.5 mV.

Also, in many cases, a layer of SAM was assembled on the surface of Au before coating it with polypyrrole. SAM - 11-(1H-Pyrol-1-yl)-undecan-1-thiol monolayer, which was formed according to the following procedure: 25 μl of 1 mM PUT in EtOH solution was added to an SPR cuvette filled with EtOH solvent and left for 14 hours. After that, the surface was washed several times with EtOH solvent, finally changing it to PBS solution.

All experiments were repeated at least 5 times.

2. RESULTS AND DISCUSSION

2.1. Synthesis of Heterogeneously Conductive Polypyrrole Layer by McDsP Method in Non-Aqueous Medium

During electropolymerization, a gradual increase in current was observed in most of the polymerization steps starting from the 2nd anodic pulse. However, during the 1st pulse, higher currents were always recorded than in the next current jump. The same effect and a similar $I_{(t)}$ development of Ppy formation were observed in previously published work [3].

And this effect was observed in all cases, but it was most expressed in 50 mM pyrrole polymerisation solution. In Figure 1, we present the chronoamperogram of the first potential pulse in $I = f(t^{-1/2})$ coordinates compared to the data of the 2nd and 3rd pulses. Applying the Cottrell equation, the slopes of the 1st, 2nd and 3rd straight lines were calculated, which are equal to 20.2 ± 0.1; 11.1 ± 0.1 and 10.9 ± 0.09 $\mu A \cdot s^{-1/2}$, respectively. As we can see, the slope of the anodic current was recorded almost twice as high during the 1st pulse as in the following cycles. Performing the cathodic potential pulse (1.0 V → 0.0 V), we obtained similar dependences in the current vs $t^{1/2}$ coordinates (Fig. 1, 1 ', 2' and 3 'curves), because the slope angles of these curves are quite similar, -4.53 ± 0.01, -5.40 ± 0.01, and -5.59 ± 0.01 $\mu A \cdot s^{-1/2}$, respectively, which shows us that the current flows less during the first cathodic jump than at the 2nd or 3rd.

However, we believe that this effect during anodic jump is related to the adsorption of pyrrole prior to its electropolymerization, as has been observed, for example, with AFM or STM techniques [4,5]. Therefore, we believe that at the non-oxidative electrode potential (in our case 0 V (Ag/AgCl)) an excess of monomer (ad-layer) may form on the Au surface, which results additional anodic current I_{ad} in oxidation process during the first anodic potential pulse (0.0 V → 1.0 V). It is likely that the relaxation time of that pyrrole ad-layer formation is greater than 10 sec, so a lower current is recorded before

the 2nd and subsequent oxidative spikes. Using the Cotrrell equation, whose slope angles are related to the surface concentration, therefore it can be initially concluded that before the 1st potential pulse, the surface pyrrole concentration could be 1.8 times higher than before the 2nd.
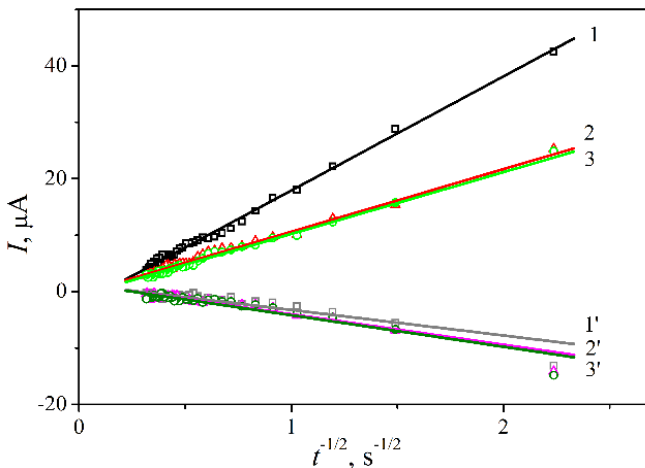

Fig 1.: Chronoamperograms (Cotrrell coordinates) obtained in AcN-TBAPF$_6$ + 50 mM pyrrole solution which were recorded during the first three anodic potential pulse: 1, 2, and 3; Chronoamperograms of 1′, 2′, and 3′ are reversible (cathodic) potential pulses.

It can also be observed that during the reversible (cathodic) potential jump (1.0 V → 0.0 V) a lower current was recorded than during the anodic step. Comparing the 2′, 3′ lines shown in Figure 1 with the line 2 and line 3, it can be observed that during the 1.0 V → 0.0 V pulse $I = f(t^{-1/2})$ functions slope is on average 2.01 times less than 0.0 V → 1.0 V during the potential pulse. We explain this by the fact that the anodic current I_a possibly consists of three components: Double electric layer charge I_{dl}, pyrrole oxidation I_{py}, and Ppy oxidation I_{ppy+} currents: $I_a = I_{dl} + I_{py} + I_{ppy+}$. Meanwhile, the cathodic

current occurs only due to double electric layer recharge I_{dl}, and due to the reversible reduction of Ppy I_{ppy-}: $I_c = I_{dl} + I_{ppy-}$. Polypyrrole oxidation and reduction currents I_{ppy+} and I_{ppy-} are primarily related to the reversible formation of a charge in the polymer layer (polarons and/or bipolarons), accompanied by doping/dedoping process in the Ppy layer [6]. In addition, as demonstrated in [7] studies, overoxidation of the Ppy layer and the cross-linking of polymeric Ppy chain can take place at the same time. Both of the latter phenomena are irreversible.

Figure 2 shows our observed trend of Q_{dl} change depending on number of cycles during the oxidation-reduction process and the concentration of pyrrole in the polymerization solution. As we can see in this 3D graph, Q_{dl} grows with increasing number of oxidation-reduction steps and pyrrole concentration in solution C_{Py}.
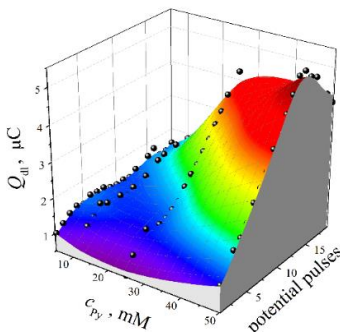

Fig 2.: The 3D diagram of the charge Q_{dl} used to fill double electric layer. Determined from the reversible potential pulses.

The probable explanation for this effect is an increase in the surface area of the electrode as the conductive Ppy layer grows. At high pyrrole concentrations (50 mM), rougher polypyrrole surfaces should form than at low concentrations (5 mM). In previous studies in our laboratory, using AFM and SEM methods, it has already been observed that the surface roughness increases with the growth of the

polypyrrole layer [8]. Similar tendencies with the AFM methodology have also been published in the work of other authors [9].

During the growth of the Ppy layer, we observed that after more than 15 oxidation-reduction pulses, Q_{dl} starts to decrease and this was most noticeable in 50 mM Py solution (Fig. 2). We believe that this phenomenon may be related to an increase in the electrical resistance of the Ppy layer. To test this hypothesis, we investigated the formation of the Ppy layer by the EIS method. Impedance spectra were recorded before polymerization (0 ox.-red pulses) and after 1, 5, 10 and 20 ox.-red pulses at C_{Py} = 5, 10, 25 and 50 mM. Prior to each experiment, the Au electrode was reconstituted (cleaned). Figure 3 shows the obtained EIS spectra in Bode coordinates.

In Figure 3, we see that the formation of a polypyrrole layer with different numbers of pulses results in EIS spectra of different forms, and this effect is manifested by increasing the concentration of pyrrole in the solution. With a higher number of pulses, an increase in the total electrical capacity of the system, which can be observed in the low frequency range (1 Hz), is recorded. Real resistance |Z| increase can also be observed in the medium frequency range (~1000 Hz) by forming a polypyrrole layer in 50 mM pyrrole solution (Fig. 3D red and purple dots).
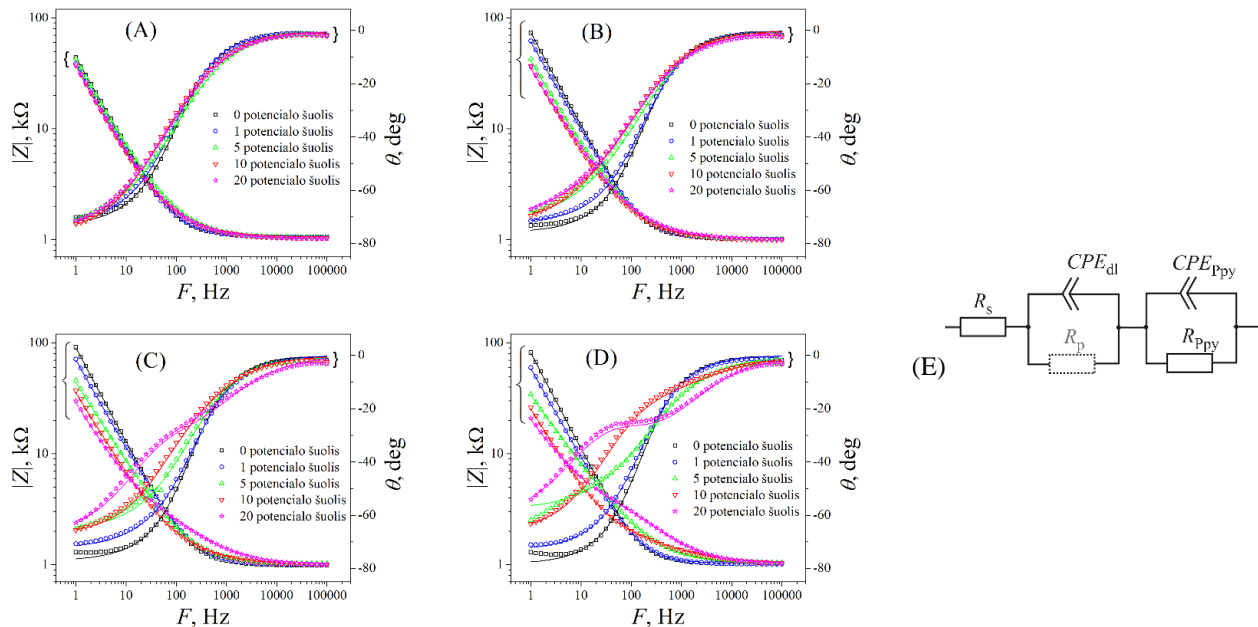
Fig. 3: EIS spectra recorded in the frequency range 1 Hz to 100 kHz at 0 V electrode potential. (A) spectra were obtained by polymerization in 5 mM Py solution, (B) - 10, (C) - 25, (D) - 50 mM Py solutions. The spectra are shown in different colours after the corresponding ox.-red. number of cycles. The continuous curves represent the theoretical data calculated using Figure 3E equivalent scheme.

As we can see from fig. 3, theoretical impedance spectra (continuous curves) quite closely describe the experimental data (the goodness of fit is in the range of $9.8 \cdot 10^{-5}$ - $8.4 \cdot 10^{-4}$).

Figure 4 shows calculated CPE_{dl} (A) and R_{Ppy} (B) data (3D diagrams). It can be noticed that the tendency of CPE_{dl} change is similar to the change of Q_{dl} (double electric layer filling charge (Fig. 2)): CPE_{dl} (like Q_{dl}) grows with increasing number of oxidation-reduction pulses and pyrrole concentration in polymerisation solution. This would not contradict our preliminary conclusion that the conductive surface area is likely to increase with the growth of the Ppy layer, and this effect is most pronounced in solutions with higher pyrrole concentrations (> 10 mM).
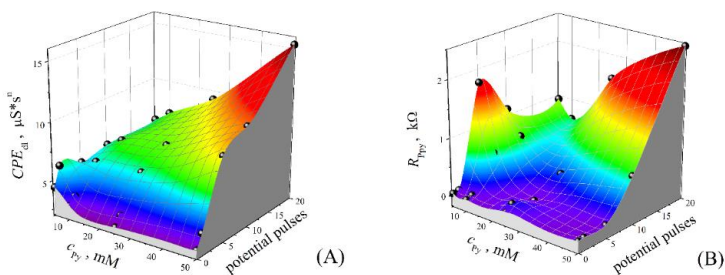

Fig. 4: A and B - the change of double layer capacity (CPE_{dl}) and Ppy layer resistance (R_{Ppy}) depending on the solution concentration and performed ox.-red. number of cycles.

In the R_{Ppy} data, as in the change of CPE_{dl}, we can notice a similar tendency. We believe that the increase in R_{Ppy} during the formation of the Ppy layer by McDsP is related to the irreversible overoxidation of the polymer. This is due to the double process: at each anodic potential pulse, in parallel with the polymerization of the pyrrole, the oxidation of the previously formed polypyrrole also takes place. This double process would also explain the decrease of Q_{dl} when more than 15 ox.-red pulses were performed in 50 mM pyrrole solution (Fig. 2). Similar

data are presented in Marchesi work [10], in which the authors explain the increase in the resistance of the Ppy layer by the degradation effect of the polymer during its overoxidation.

As it is seen from here presented investigation and some previously published data, during the electrochemical formation of Ppy, formed Ppy layer the most probably has rather uneven structure instead of forming very homogeneous film. This conclusion is in line with the statement presented in other research [11], which states that Ppy is covering Au surface according to layer-by-layer formation based principle. In addition, in our laboratory previous researches [8] we have observed that during the initial Ppy-layer formation phase "Ppy islands" are appearing. These "Ppy islands" are initially formed on the peaks of Au surface, where the electrical potential is highest, due to fundamental features, which are related to charge distribution on the surface of varying geometry. Therefore, at certain moments of charging/discharging processes much higher potential value is observed on the peaks in comparison to that observed on the flat surface.

On the basis of our investigations, we are presenting a model of Ppy-layer formation on the Au-based electrode surface (Fig. 5). In this model during polymerization process formed Ppy particles regarding to overoxidation-level are shown in different colours (from white until dark-blue). These Ppy particles are formed on electrode surface by elevated anodic potential and, due to exposition to higher anodic potentials for different duration, at different stages of polymerisation formed Ppy particles were oxidized for different durations. According to this representation: (i) particles, which are formed during the most recent anodic potential step, are indicated in white colour (ii) these particles, which were oxidized by several potential pulses, are indicated in bluish colour and (iii) particles, which were treated by maximal number of anodic potential pulses, are indicated in dark-blue colour. Due to longest exposure to high potential the last particles were the most significantly oxidized. During the formation of Ppy layer, when potential is increasing/decreasing in the range from 0.0 V up to

1.0 V and back, mixed Ppy based particle islands are gradually formed. In this model we can distinguish two very distinct cases: (i) the formation of Ppy from very low pyrrole concentration (5 mM) based polymerization bulk solution, (ii) the formation of Ppy from high pyrrole concentration (50 mM) based polymerization bulk solution. In the first case - after n pulses, on Au surface Ppy structures with varying conductivity are formed, therefore, electrode is not blocked by Ppy-structures of low conductivity, which are depicted as dark-blue particles/areas. In the second case, at higher pyrrole concentrations in polymerization bulk solution, the structure of formed Ppy layer is more evenly distributed and then the Ppy layer is formed according to layer-by-layer formation principle as it has been reported in other research [11]. In such case finally all Au-electrode surface is evenly blocked by badly conducting overoxidized Ppy layer, therefore, the highest overoxidation level of Ppy-based particles is observed directly on Au electrode surface. At the same time, newly formed more conducting Ppy particles are formed on the boundary between Ppy layer and polymerization solution and in such way newly formed Ppy particles increase electrochemically active surface area of electrode. This effect explains the increase of CPE_{dl} value, which is observed by the increasing number of anodic potential pulses.

Py concentration in AcN-TBAPF6 polymerization bulk solution

ox.-red. potential pulses
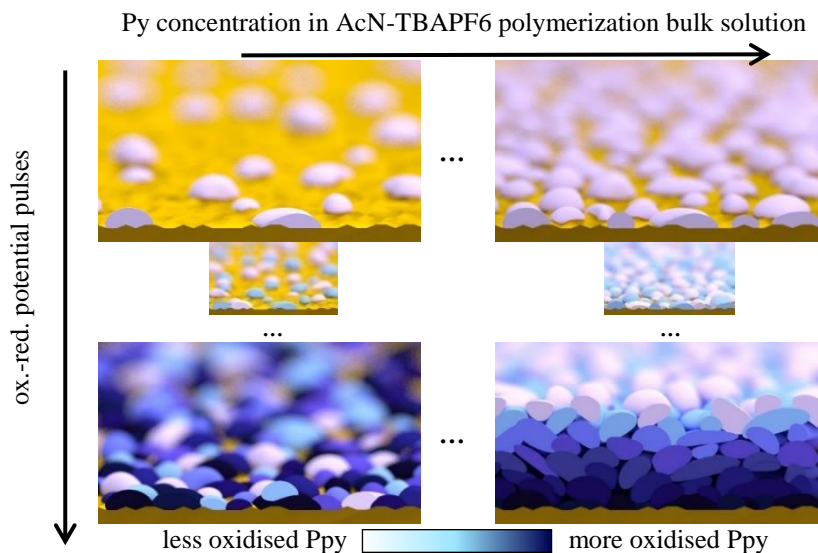
less oxidised Ppy ▢ more oxidised Ppy

Fig. 5: Estimated model of Ppy-layer formation on Au electrode during the course of potential pulse based electrochemical polymerization of pyrrole, at X coordinate the concentration of pyrrole and at Y coordinate a number of applied potential pulses are represented. Darker colours represents higher polypyrrole oxidation level, which was achieved by longer explosion towards high electrode potentials.

Our EIS measurements indicated that by progressing film deposition significantly increases the value of R_{Ppy} (Fig. 4B). Hence, here presented model (Fig. 5) is also supported by some experimental data, which were gathered using current-sensing based AFM method (CS-AFM). Here presented model (Fig. 5) well explains the fact why from EIS spectra calculated resistance R_{Ppy} (Fig. 4B) is higher in such cases when Ppy is formed from polymerization solutions containing higher concentrations of pyrrole.

2.2. Synthesis and investigation of molecular glyphosate imprints in polypyrrole matrix by ESPR method

Thus, after studying the peculiarities of Ppy layer formation, we found that by increasing the concentration of pyrrole in the polymerization solution and / or increasing the number of chronoamperometric pulses applied during polymerization, we obtain a mixed, overoxidized layer with lower conductivity properties. On the other hand, the layer obtained by electropolymerization in a 5 mM pyrrole solution has more heterogeneous conductivity properties. This fact became one of the reasons why we performed electrosynthesis of the MIP sensor from a 10 mM pyrrole polymerization solution with only one chronoamperometric pulse. Another reason for this is the sensitivity of our chosen SPR method. In order to study the formed MIP layers with a sufficiently sensitive method that could tell us with sufficient accuracy about the polymer-analyte interactions, we chose the ESPR analysis method. However, by performing layer synthesis from polymerization solutions with higher pyrrole concentrations or by applying more pulses, the jump of the SPR signal was obtained too large, going outside the measurement range.

Also, comparing the data with the studies performed in the bachelor's thesis when the electrosynthesis of polypyrrole was performed in aqueous media, we decided to carry out further studies in PBS buffer solution. Also, we selected a low acetonitrile-soluble glyphosate analyte as the subject of our study.

The typical chronoamperograms of MIPpy and NIPpy formation on the bare Au electrode or on SAM/NIPpy and SAM/MIPpy are listed in figure 6E. The initial point in time of the onset of polymerization the registered charging current value depends on the electrical double layer capacitance at the Au electrode interface with surrounding polymerization solution. It was observed that the highest current value was registered at the bare Au electrode in the interface with PBS_{Py} polymerization bulk solution. The current value at the same bare Au electrode but in the interface with PBS_{Py+Gly} polymerization bulk

solution was slightly lower. In previous publication it was stated that the main limitation for electrochemical detection of glyphosate is the lack of electroactivity of the molecule [12]. Hence, it was expectable to have such lower current in time on the onset of MIPpy polymerization. The current values on the onset of polymerization at the PUT treated Au electrode in the interface from the PBS_{Py} and PBS_{Py+Gly} polymerization bulk solutions was 25 and 5 times lower. Such lower current registered during the onset of polymerization implicit that the SAM on the surface forms the barrier for pyrrole molecules.
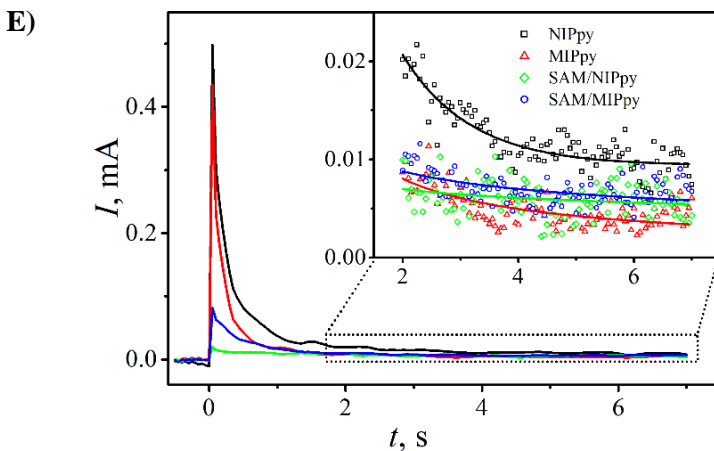
E)
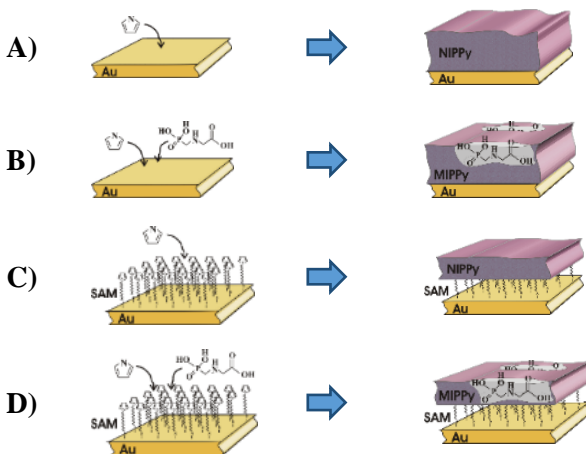
Fig. 6: The chronoamperometric deposition of MIPpy and NIPpy on the top of Au electrode. The expected scheme for the formation: A) of NIPpy and B) of MIPpy on the bare ESPR-sensor; C) of SAM/NIPpy and D) of SAM/MIPpy on the ESPR-sensor treated with SAM. E) The typical chronoamperograms obtained during the application of a single potential pulse of 1 V vs Ag/AgCl for 7 s. For the deposition of NIPpy was used PBS_{Py} polymerization solution containing 10 mM of pyrrole in PBS and for the deposition of MIPpy the PBS_{Py+Gly} polymerization bulk solution containing 10 mM of pyrrole and 1 mM of glyphosate in PBS was used. The temperature was kept constant at 298.0 ± 0.5 K.

The inset in the figure 6E demonstrates an enlarged view of current changes during polymerization of NIPpy and MIPpy or SAM/NIPpy and SAM/MIPpy films from 2nd second to the end of the polymerization. Several processes may be taken into account at this stage of polymerization. These are diffusion, the rate of film formation, and charge transfer across the phase boundary. In this study it was observed, that the highest electric current flows through the electrode when NIPpy is formed. In the case of SAM/NIPpy and SAM/MIPpy deposition the electric current values become so similar, that the differences between them become negligible. The lowest electric current flows through the electrode when MIPpy is deposited.

Such differences of the electric current inspired to take the closer look to this phenomenon.

During the formation of both MIPpy and NIPpy layers we integrated registered current in time and provided the results in Q vs $t^{1/2}$ coordinates (Fig. 6). When 1 sec. passed after applied potential pulse the dependence Q vs $t^{1/2}$ becomes linear. For these linear parts of curves we have applied tangent-lines (Fig. 6, tangent-lines), the slope of these tangent lines assessed by integrated Cottrell equation (Anson plot) [13] is describing redox processes that are taking part during anodic process. In addition to electrical current measurements, which were performed during electrochemical deposition, SPR measurements were performed in parallel (Fig. 6 solid figures).
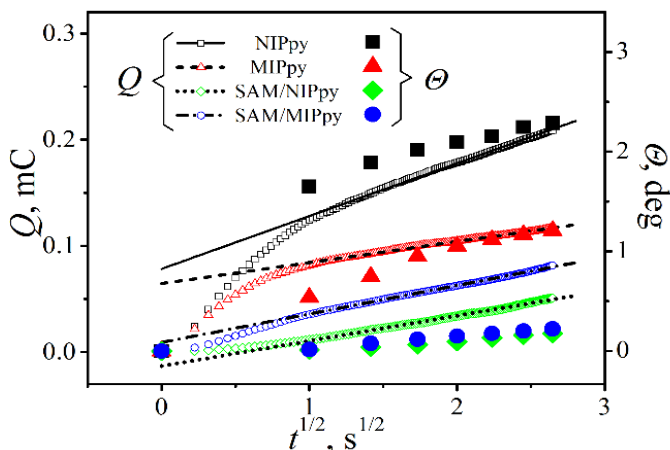

Fig. 6: The typical deposition curves of MIPpy, NIPpy, SAM/MIPpy, and SAM/NIPpy expressed in electrical charge Q vs $t^{1/2}$, which was calculated from chronoamperometry data presented in Fig. 5E. The hollow symbols represent charge passed and straight lines indicates the tangents of charge passed. Tangents were drawn after the first second. Solid figures are the SPR signal Ө which was observed in parallel.

Figure 6 illustrates that SPR measurements are well correlating with electrochemical data. Using both SPR method and chronoamperometrically determined passed charge registration

approach, it was determined that if the same electrochemical parameters are applied for electrochemical polymerization of pyrrole, then thicker Ppy layer is formed when electrodeposition of NIP is performed on bare ESPR-sensor surface (Fig. 6 black curve). Moreover, the Ppy-based layer in PBS_{Py} polymerization bulk solution is formed much efficiently in comparison to that in PBS_{Py+Gly} solution (Fig. 6 red curve). This phenomenon is related to pre-adsorption of glyphosate to ESPR-sensor [14], which partly insulate and passivate initially active electrochemically available surface of ESPR-sensor. When the electrodeposition is performed on ESPR-sensor that is pre-modified by PUT based SAM, and then we are observing much lowed differences in SPR signal. This can be related to the formation of thinner Ppy layer, because formed SAM reduces the charge transfer efficiency and, therefore, at the same electrochemical conditions lower amount of Ppy is formed on the SAM-coated ESPR-sensor surface. Lower amount of passed charge is well indicated by blue and green curves in figure 6. In addition, it should be noted, that during the formation of SAM/MIPpy the amount of passed charge is higher in comparison to that passed during the formation of SAM/NIPpy layer. During the formation of SAM/MIPpy layer much more porous Ppy layer is formed on the surface of SAM due to within Ppy entrapped molecules of glyphosate, which in PBS, pH 7.0, are in the form of $O_2CCH_2N^+H_2CH_2PO_3^{2-}$ ion [15] and, therefore, they can act as a charge carrier.

Aforementioned chronoamperometric investigations revealed that the presence of glyphosate is significantly influencing the efficiency of electrochemical deposition of Ppy. Therefore, in order to understand better this phenomenon, we have performed EIS measurements. EIS was registered in-situ instantly after the synthesis of the corresponding Ppy layer and refilling of ESPR cell by PBS solution.

We have presumed that our system has two main phase boundaries, one between solution and Ppy and another one between Ppy or SAM and Au-based electrode surface. Taking into account above-mentioned

27

presumption, according to first approximation we have applied electrical circuit, which is presented in the inset of figure 7.

In this equivalent circuit constant phase element (CPE_{dl}) represents the capacitance of double electrical layer at phase boundary between solution and polymer based layer, and element (C_l) is related with capacitance, which is formed between polymer layer and electrode. Charge transfer resistances trough phase boundaries are described by corresponding equivalent circuit elements between solution-polymer (R_p) and polymer-electrode (R_{Ppy}). In such way R_{Ppy} could be associated with the resistance of conducting polymer layer [16]. In these our calculations we have assumed that not compensated solution resistance R_S is described by constant value of $117.0 \pm 1.4\ \Omega$.

The black curves of figure 7 illustrates that using here described calculated EIS spectra well fits with experimental data with a goodness of fit within $8.4\cdot10^{-4} - 7.4\cdot10^{-3}$ interval.
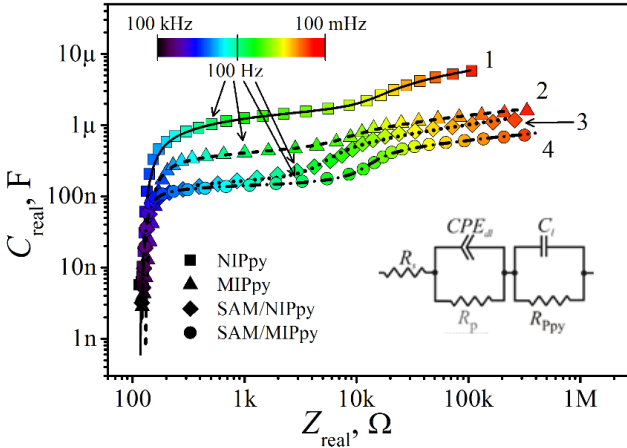

Fig. 7.: Electrochemical impedance curves of MIPpy-, NIPpy-, SAM/MIPpy- and SAM/NIPpy-modified ESPR-sensors; EIS spectra registered in the frequency range of 0.1 Hz–100 kHz, at 0 V *vs* Ag/AgCl$_{(satur.)}$, alternating potential amplitude was 10 mV and 10 points per decade were registered. **Inset**: equivalent electrical circuit applied for the assessment of EIS spectra.

We think that for NIPpy both capacitances C_{dl} and C_l higher values is related with that during the formation of NIPpy layer, thicker layer of Ppy is formed and therefore it has greater electrochemically active surface area in if compared with that of formed MIPpy layer. It should be noted that in these cases, when SAM-based layer was formed on the electrode before the deposition of Ppy layer, we have observed lower double layer capacitance C_{dl}, because at phase boundary the formation of 'thicker' dielectric layer in the form of SAM was observed.

These data illustrate that SAM layer decreases charge transfer efficiency from solution to ESPR-sensor surface. For the same reason the oxidation of pyrrole is hindered over ESPR-sensor that are modified by SAMs and, therefore, lower amount of Ppy is formed and deposited over SAM-modified electrodes. Rather similar conclusion was presented in some researches by other authors [17,18].

It should be noted that R_p for MIPpy layer is about 2.8 times greater than that for NIPpy layer. Such hindrance of charge transfer in the case of MIPpy layer can be related to intercalation/association between glyphosate and Ppy. Glyphosate at neutral pH is ionized and is present in the form of Gly^{2-} anion. Therefore, in Ppy matrix this ion can reduce the mobility of polarons and bipolarons and in such way to reduce charge transfer within backbone of this conducting polymer. This prediction is in line with effect, which was observed when the interaction between chlorophosphon azoIII and UO^{2+} was investigated by EIS-based method [16].

However, we think that the increase in the electrical resistance of the system is induced by interaction of glyphosate with surface of ESPR-sensor. The decrease of diffusion current observed during the formation of Ppy from PBS_{Py+Gly} polymerization bulk solution we attributed to blocking of ESPR-sensor by adsorbed glyphosate molecules. The increase of resistance after the formation MIPpy layer can be also related to adsorption of glyphosate to ESPR-sensor surface.

The adsorption of the glyphosate on the bare ESPR-sensor was evaluated by the CV when the potential was swept from -0.4 V to +1.25 V (Fig. 8). To achieve this goal two solutions were used to perform the CV measurements: the first CV was recorded in PBS without glyphosate. During the next step, the glyphosate was added to the PBS (PBS$_{Gly}$) and the CV was recorded repeatedly. In figure 8 the typical cyclic voltammograms of PBS and PBS$_{Gly}$ (C_{Gly} is 0.5 mM) are demonstrated. The evaluation of changes in the peaks currents and position in these cyclic voltammograms leads to the conclusion that glyphosate is rather strongly adsorbed on the bare ESPR-sensor.
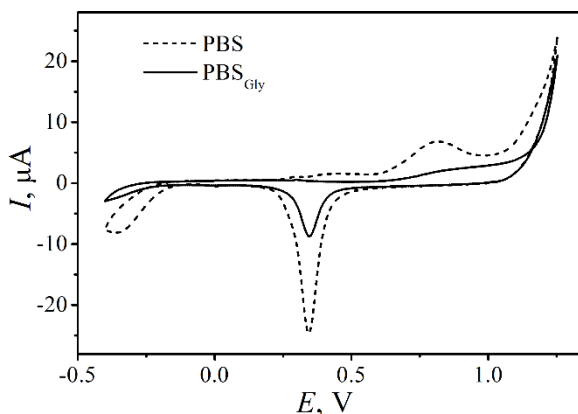

Fig. 8. Cyclic voltammetry based evaluation of glyphosate adsorption on the bare ESPR-sensor. The potential was alternated from -0.4 V to +1.25 V, at a step potential of 3.5 mV and a scan rate of 50 mV/s. Potential was cycled in two solutions pure PBS and PBS$_{Gly}$ with glyphosate at the concentration of 0.5 mM.

It was determined, that the oxygen desorption charge in PBS solution was approx. 39.8 μC and in PBS$_{Gly}$ solution approx. 11.8 μC when potential was changed from positive (anodic) to more negative. This suggests concluding that the active layer of ESPR-sensor in PBS$_{Gly}$ with C_{Gly} = 0.5 mM was reduced by a factor of 3.4 times in comparison with the CV results observed in PBS. This reduction of

the active layer of the ESPR-sensor causes that the adsorption of oxygen is more impeded.

The obtained results of the glyphosate and Py adsorption induced to remodel the preliminary formation model of MIP with glyphosate imprints from the model demonstrated in figure 6B to the model demonstrated in figure 9. We consider, that glyphosate on the bare ESPR-sensor tends to form the non-uniform layer. The molecules of SAM due to their structure on the Au of ESPR-sensor surface form the uniform and well-ordered films [19]. Meanwhile there is no proof about the ability of the glyphosate to form such uniform structure. The obtained data reveals that the glyphosate molecules tend to adsorb on the Au of ESPR-sensor surface, but though these adsorbed interfering molecules, the polymerization of Ppy on the bare ESPR-sensor still occurs.
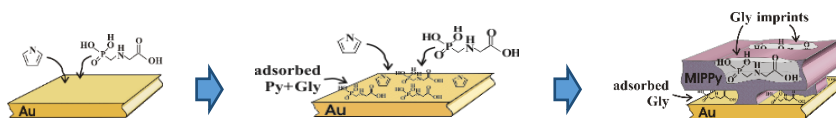

Fig. 9: The model of the formation of the MIPpy with glyphosate (Gly) imprints.

The aim of this part of the experiments was to determine which formed structure is mostly suited for the determination of glyphosate. For this reason, ESPR-sensors modified by all structures (Fig. 6, A-D) were 90 seconds 'washed' by PBS (Fig. 10, *step 1*). In such way experimental conditions for the formation of NIPpy- (Fig. 6, A and C) and MIPpy-based (Fig. 6, B and D) layers were unified, moreover, by here mentioned procedure template molecules were removed from MIPpy. Injected PBS_{Gly} concentration was 0.2 mM, which was by 5 times lower in comparison to that used for the formation of MIPpy layers. After this the layers were additionally washed and again EIS spectra were registered step 3 (Fig. 10). Typical sensograms are presented in figure 10.
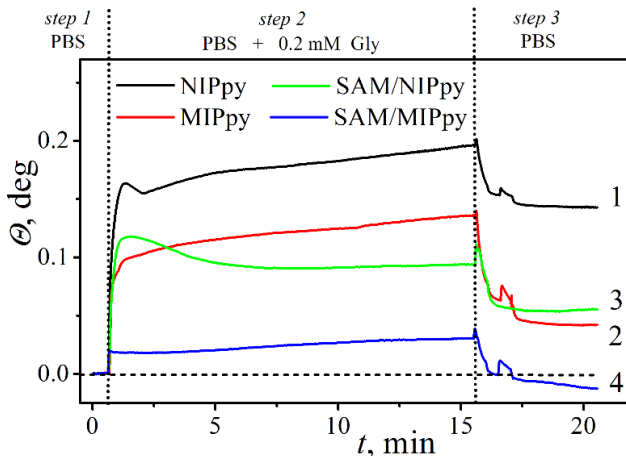
Fig. 10: SPR signals determined for NIPpy (1), MIPpy (2), SAM/NIPpy (3) and SAM/MIPpy (4) layers in different solutions: step 1 – bare PBS; step 2 – PBSGly where CGly = 0.2 mM; step 3 – bare PBS.

After the injection of PBS$_{Gly}$ solution into SPR cell (*step 2*) rapid increase of SPR signal was determined, which can be associated with variation of composition and association of Gly with corresponding layer. The highest increase was observed when solution was injected into the system in which electrode was modified by NIPpy and the lowest one for electrode modified by SAM/MIPpy. It should be noted that after injection of PBS$_{Gly}$ solution into SPR cell with surfaces modified by NIPpy and SAM/NIPpy layer in all cases we have observed the 'jump' of SPR signal (Fig. 10 black (1) and green (3) curves), which after this decreases rather fast, but this effect was not observed when surfaces modified by MIPpy and SAM/MIPpy layers were investigated (Fig. 10 red (2) and blue (4) curves). We predict that this effect is related with the fact that after the injection glyphosate molecules are penetrating deeper into MIPpy- and SAM/MIPpy-based layers where they are forming complexes with imprinted sites, but in the case of similar investigations with NIPpy- and SAM/NIPpy-

modified surfaces on boundary between polymer and solution steady-state conditions are reached much faster.

It should be noted that SPR signal for both MIPpy- and NIPpy-modified ESPR-sensors has constantly increased during the course of multiple measurements, which most probably illustrated that neither MIPpy-, nor NIPpy-layers were saturated by glyphosate, while in the case of SAM/MIPpy- and SAM/NIPpy-modified layers' stabilization of SPR signal was observed after rather short period of time (15 minutes). During later phase of experiments, when PBS_{Gly} is exchanged by bare PBS (*step 3*) we have observed that the rate of dissociation/desorption of glyphosate from both Ppy-based layers is rather different. Therefore, it is expected that part of glyphosate molecules remains adsorbed on SAM/MIPpy- and SAM/NIPpy-based layers.

Registered SPR data were modelled, assessed and fitted by software „Kinetic Evaluation". The fitting of experimental and theoretically calculated provided dissociation rate constants k_a and k_d. The ratio of these constants provided us equilibrium constant (K_D) for the reaction:

$$PPyGly \underset{k_a}{\overset{k_d}{\rightleftarrows}} PPy + Gly \qquad (1)$$
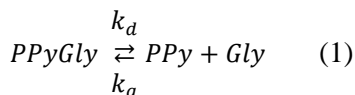
Using values of dissociation constant (K_D) for the reaction 1 we can easily determine free energy of Gibbs (ΔG_0) for glyphosate association with corresponding layer [20]:

$$\Delta G^0 = RTlnK_D \qquad (2)$$

Calculated ΔG values (table 1), illustrate that glyphosate is interacting with ESPR-sensor's surface much stronger in comparison to the interaction with Ppy. The same fact is confirmed by calculations of desorbed analyte, which was rather low and was calculated according this equation:

$$D_\% = \frac{\theta_{PBSGly} - \theta_{PBS}}{\theta_{PBSGly}} \times 100 \qquad (3)$$

where Θ_{PBS} SPR measurement value in PBS solution and Θ_{PBSGly} SPR signal value in PBS_{Gly} solution.

This calculation illustrates that interaction of glyphosate with NIPpy and MIPpy, respectively -21.68 ± 0.20 and -19.51 ± 0.15 kJ/mol. As we can see from result presented in table 1, after the interaction of glyphosate with SAM/MIPpy, the regeneration of SAM/MIPpy-modified ESPR-sensors is the most efficient and during first regeneration cycle it reaches 89 %. It is worth to note that quantitatively the regeneration of ESPR-sensors modified by NIPpy, SAM/NIPpy and SAM/MIPpy layer is rather similar, about 50 m°. Exception is ESPR-sensors modified by MIPpy, because for this ESPR-sensor's $\Delta\Theta$ value increases more than twice of that determined for other three before mentioned ESPR-sensors. This effect illustrate that the regeneration of MIPpy-modified ESPR-sensor is rather efficient.

Table 1. The reversibly of SPR signal and calculation of kinetic characteristics, which were determined during *step 2* → *step 3* experiment. For comparison the evaluation was also performed on clean ESPR-sensor.

Surface	$\Theta_{PBSGly} \pm e$, m°	$\Theta_{PBS} \pm e$, m°	D, %	$k_a \pm e$, $M^{-1}sec^{-1} *10^3$	$k_d \pm e$, $sec^{-1} *10^{-2}$	$K_D \pm e$, $*10^{-5}$	ΔG^0, kJ/mol
Au	170.0 ± 39.1	123.4 ± 28.4	27.4	2.88 ± 0.03	4.83 ± 0.13	1.68 ± 0.06	-27.26 ± 0.10
NIPpy	200.7 ± 8.0	150.6 ± 63.7	25.0	0.36 ± 0.02	5.72 ± 0.17	15.89 ± 1.20	-21.68 ± 0.20
MIPpy	173.8 ± 82.5	67.3 ± 13.3	61.3	0.25 ± 0.01	9.45 ± 0.08	38.18 ± 2.33	-19.51 ± 0.15
SAM/NIPpy	84.5 ± 8.7	44.0 ± 5.8	47.9	0.45 ± 0.01	1.73 ± 0.11	3.84 ± 0.34	-25.20 ± 0.24
SAM/MIPpy	58.2 ± 35.8	6.3 ± 3.1	89.2	1.35 ± 0.09	6.01 ± 0.32	4.44 ± 0.52	-24.84 ± 0.30

After the replacement solution in ESPR cell EIS measurement was performed. For the interpretation of EIS spectra we have applied the same equivalent circuit that is presented in figure 7 and has been discussed above. In table 2 characteristics of equivalent circuit, which were calculated by fitting calculated spectra are presented. These characteristics of equivalent circuit illustrate that glyphosate has the most significant influence for EIS-characteristics of MIPpy- and NIPpy-modified ESPR-sensors, which are not pre-modified by SAM layers. On the other hand, some characteristics of equivalent circuit are tending to get initial value when glyphosate is removed from ESPR-cell, e.g.: R_p of NIPpy-modified ESPR-sensor in glyphosate containing PBS$_{Gly}$ solution increases by 39.5%, but when glyphosate is removed from ESPR-cell remains only 31.6% of here mentioned R_p increase. Meanwhile, R_p of MIPpy-modified ESPR-cell after incubation in PBS$_{Gly}$ solution increases by 78.4%, but after removal of glyphosate it retains initial value (inaccuracy is 8%). This is positive result, which illustrate partial regeneration of MIPpy layer.

But it should be noted that in the case of NIPpy- ir MIPpy-modified ESPR-sensors some characteristics are changing irreversibly. When we have exchanged solution in ESPR-cell (Step 1 → Step 2 → Step 3) C_l, then the capacitance, which is associated with Ppy/Au phase boundary for NIPpy-modified ESPR-sensor decreased by 1.9 times and for MIPpy it decreased by 1.2 times.

The value of capacitance C_{dl} for NIPpy is lower by 1.2 times, but for MIPpy it increases a little bit. It should be noted, that for both SAM/NIPpy and SAM/MIPpy the capacitance C_{dl} increases not significantly. We think that this result is observed due to several reasons: (i) on pre-deposited SAM layer much thinner Ppy layer is formed in comparison to that formed on bare ESPR-sensor, therefore, characteristics, which are describing equivalent circuit applied for the evaluation of EIS spectra are changing less significantly; (ii) another reason is related to the diffusion of glyphosate within Ppy layer. In the case of NIPpy-modified ESPR-sensor it is expected that some

glyphosate molecules can diffuse deeply within Ppy layer and even reach gold layer surface. Therefore, the EIS equivalent circuit characteristics are not recovering back to initial values when glyphosate is removed from ESPR-cell. The SAM/NIPpy-modified ESPR-sensor is less sensitive towards glyphosate because SAM-based under-layer is blocking glyphosate from gold surface.

According to our opinion, during the formation of MIP-based glyphosate sensors it is important to take into account possible glyphosate diffusion and adsorption directly on gold of ESPR-sensor surface. As we have shown in our research this problem can be solved by several methods: (i) by the formation of SAM-based under-layer between gold and electrochemically deposited MIPpy layer, but in this case it is important to take into account isolating property of SAM-based under-layer, because this property reduces electrodeposition rate of Ppy; (ii) another alternative method to protect the gold surface of ESPR-sensor from negative influence of glyphosate could be based on formation of NIPpy-based under-layer, which is covered by MIPpy. Some researchers are applying the strategy based on the formation of thin NIPpy-based under-layer before the formation of MIPpy-based sensing layer. Such system was applied for the determination of flumequine (FLU) using surface acoustic wave (SAW) signal transduction system [21], where authors by experimentally and by density functional theory (DFT) based calculations have determined that FLU molecules are forming complexes with the surface of gold and are blocking electrochemically active surface of gold-based electrode. Therefore, in order to avoid this unwanted effect before the formation of MIP-Ppy layer authors have deposited thin NIPpy under-layer, which enabled adhesion of MIPpy layer.

Table 2. The parameters of equivalent electrical circuit elements calculated for ESPR-sensor modified with MIPpy and NIPpy or SAM/MIPpy and SAM/NIPpy at different steps of the experiment (*Step 1 → Step 2 → Step 3*).

Surface	**Electric parameter**	*Step 1* **PBS**	*Step 2* **PBS$_{Gly}$**	*Step 3* **PBS**
NIPpy	$R_p \pm$ **e, MΩ**	3.8 ± 1.4	5.3 ± 2.2	5.0 ± 2.0
	$R_{Ppy} \pm$ **e, kΩ**	7.1 ± 0.5	8.2 ± 0.4	7.5 ± 0.4
	$C_{dl} \pm$ **e, nF**	457 ± 6	357 ± 4	372 ± 4
	$\alpha \pm$ **e**	0.780 ± 0.002	0.772 ± 0.002	0.776 ± 0.002
	$C_l \pm$ **e, nF**	5451 ± 261	2544 ± 89	2914 ± 110
MIPpy	$R_p \pm$ **e, MΩ**	11.1 ± 2.9	19.8 ± 9.0	10.2 ± 2.2
	$R_{Ppy} \pm$ **e, kΩ**	3.8 ± 0.3	3.5 ± 0.3	4.3 ± 0.3
	$C_{dl} \pm$ **e, nF**	250 ± 2	222 ± 2	282 ± 3
	$\alpha \pm$ **e**	0.839 ± 0.003	0.831 ± 0.003	0.858 ± 0.003
	$C_l \pm$ **e, nF**	1735 ± 111	1657 ± 110	1399 ± 74
SAM/NIPpy	$R_p \pm$ **e, MΩ**	-	-	-
	$R_{Ppy} \pm$ **e, kΩ**	3.0 ± 0.1	2.9 ± 0.1	2.7 ± 0.1
	$C_{dl} \pm$ **e, nF**	149 ± 2	148 ± 2	142 ± 1
	$\alpha \pm$ **e**	0.811 ± 0.003	0.814 ± 0.003	0.812 ± 0.03
	$C_l \pm$ **e, nF**	402 ± 15	398 ± 15	431 ± 17
SAM/MIPpy	$R_p \pm$ **e, MΩ**	-	-	-
	$R_{Ppy} \pm$ **e, kΩ**	9.1 ± 0.3	8.6 ± 0.3	8.5 ± 0.3
	$C_{dl} \pm$ **e, nF**	159 ± 2	159 ± 2	160 ± 2
	$\alpha \pm$ **e**	0.865 ± 0.003	0.869 ± 0.003	0.869 ± 0.003
	$C_l \pm$ **e, nF**	305 ± 9	297 ± 9	303 ± 9

CONCLUSIONS

1. We found that the electrical properties of the Ppy layer depend quite significantly on the concentration of monomer in the polymerization solution. The obtained results allow to assume that a certain pyrrole ad-layer is formed on the electrode surface before oxidation process.
2. During the longer formation of the Ppy layer, we observed an increase in the capacity of the double electric layer, which is related to the increase in the surface area (roughness) of the conductive polymer.
3. The change in EIS spectra showed that the reactive resistance of the electrochemical system changes with the formation of the Ppy layer. We believe that this is related to the processes of Ppy overoxidation and cross-linked polymer chain formation.
4. Electrochemical and surface plasmon resonance studies showed that the formation of NIPpy and MIPpy coatings is significantly influenced by the presence of SAM on the Au electrode surface. The presence of SAM reduces the electric charge flow during pyrrole oxidation, which suggests that the thinner Ppy layer has formed.
5. It was found that the presence of glyphosate in the initial polymerization solution complicated the electrochemical formation of the Ppy layer. We attributed this phenomenon to the competitive adsorption of glyphosate molecules compared to pyrrole on the Au surface. Adsorption of glyphosate on the electrode surface was confirmed by electrochemical and surface plasmon resonance studies.
6. SPR and EIS studies have shown that glyphosate interacts more strongly with the NIPpy layer than with MIPpy. However, we found that the interaction with MIPpy is more reversible, indicating better regeneration of the potential sensor.

LIST OF PUBLICATIONS AND CONFERENCES

List of publications:

- D. Plaušinaitis, **D. Balčiūnas**, A. Ramanavičius, Synthesis of *Heterogeneously Conductive Polypyrrole Layer from Non-Aqueous Solution Using The Double-Step Potential Technique*. Journal of The Electrochemical Society, 2020. **167**(8): p. 086510.
- V. Ratautaitė, U. Samukaitė-Bubnienė, D. Plaušinaitis, R. Bogužaitė, **D. Balčiūnas**, A. Ramanavičienė, G. Neunert, A. Ramanavičius, *Molecular Imprinting Technology for Determination of Uric Acid*. International Journal of Molecular Sciences, 2021. **22**(9): p. 5032.
- **D. Balčiūnas**, D. Plaušinaitis, V. Ratautaitė, A. Ramanavičienė, A. Ramanavičius, *Towards Electrochemical Surface Plasmon Resonance Sensor Based on the Molecularly Imprinted Polypyrrole for Glyphosate Sensing*. (Sent to Jounal).

List of conferences:

- **D. Balčiūnas**, D. Plaušinaitis, Study of Pyrrole Adsorption and Electropolymerization on Au Surface from Acetonitrile Solutions, 9th Nano-conference „Advances in Bioelectrochemistry and Nanomaterials", Vilnius, 2016.
- **D. Balčiūnas**, D. Plaušinaitis, Study of Pyrrole Adsorption and Electropolymerization on Au Surface from Acetonitrile Solutions, 19th International Conference-School "Advanced Materials and Technologies 2017", Palanga, 2017.
- **D. Balčiūnas**, D. Plaušinaitis, Study of Pyrrole Adsorption and Electropolymerization on Au Surface from PBS Solutions by using ESPR method, Open Readings 2018, Vilnius, 2018.
- **D. Balčiūnas**, D. Plaušinaitis, Study of Pyrrole Adsorption and one pulse Electropolymerization on Au Surface using ESPR

method, 20th International Conference-School "Advanced Materials and Technologies 2018", Palanga, 2018.

- **D. Balčiūnas**, D. Plaušinaitis, Study of Glyphosate Adsorption on Thin Polypyrrole Layer and on 11-(1H-Pyrrol-1-yl)undecane-1-thiol SAM Formed Polypyrrole and Comparison, Open Readings 2019, Vilnius, 2019.
- **D. Balčiūnas**, D. Plaušinaitis, Study of sensitivity to Glyphosate. Comparison of differently coated gold surfaces by using ESPR method, 21st International Conference-School "Advanced Materials and Technologies 2019", Palanga, 2019.
- **D. Balčiūnas**, D. Plaušinaitis, Synthesis and investigation of molecularly imprinted glyphosate in polypyrrole matrix by ESPR method, 22nd International Conference-School "Advanced Materials and Technologies 2020", Palanga, 2020.

CURRICULUM VITAE

Domas Balčiūnas

Education:

2010 – 2014 Bachelor of Chemistry, Vilnius University;
2014 – 2016 Master of Chemistry, Vilnius University;
2016 – 2020 Doctoral studies of Chemistry, Vilnius University.

Work Experience:

2014.09 – 2016.03 Chemist at National Public Health Surveillance Laboratory;
2016.03 – 2021.08 Sales Engineer at JSC "Tek Know Baltic";
2021.08 – Present, Head of Sales of Chemical Analysis Equipment at JSC "Tek Know Baltic".

REFERENCES

1. Ragaliauskas, T., et al., *Fast formation of low-defect-density tethered bilayers by fusion of multilamellar vesicles*. Biochimica et Biophysica Acta (BBA)-Biomembranes, 2017. **1859**(5): p. 669-678.

2. Trasatti, S. and O. Petrii, *Real surface area measurements in electrochemistry. Pure and applied chemistry*, 1991. **63**(5): p. 711-734.

3. Ramanavicius, A., Y. Oztekin, and A. Ramanaviciene, *Electrochemical formation of polypyrrole-based layer for immunosensor design*. Sensors and actuators B: Chemical, 2014. **197**: p. 237-243.

4. Marandi, M., et al., *AFM study of the adsorption of pyrrole and formation of the polypyrrole film on gold surface*. Electrochemistry communications, 2010. **12**(6): p. 854-858.

5. Khairunnisa, A., W. Liao, and S. Yau, *Adsorption and electrochemical polymerization of pyrrole on Au (100) electrodes as examined by in situ scanning tunneling microscopy*. The Journal of Physical Chemistry C, 2016. **120**(46): p. 26425-26434.

6. Diaz, A.F., et al., *Electrochemistry of conducting polypyrrole films*. Journal of electroanalytical Chemistry and Interfacial electrochemistry, 1981. **129**(1-2): p. 115-132.

7. Otero, T.F., M. Marquez, and I.J. Suarez, *Polypyrrole: Diffusion coefficients and degradation by overoxidation*. The Journal of Physical Chemistry B, 2004. **108**(39): p. 15429-15433.

8. Plausinaitis, D., et al., *Electrochemical polypyrrole formation from pyrrole 'adlayer'*. Physical Chemistry Chemical Physics, 2017. **19**(2): p. 1029-1038.

9. Chen, W., et al., *In situ AFM study of electrochemical synthesis of polypyrrole/Au nanocomposite*. Electrochemistry communications, 2008. **10**(9): p. 1340-1343.

10. Marchesi, L., et al., *Investigation of polypyrrole degradation using electrochemical impedance spectroscopy*. The Journal of Physical Chemistry B, 2011. **115**(31): p. 9570-9575.

11. Grzeszczuk, M., J. Kalenik, and A. Kępas-Suwara, *Phase boundaries in layer-by-layer electrodeposited polypyrrole resulted from 2D–3D growths of polymer sublayers*. Journal of Electroanalytical Chemistry, 2009. **626**(1-2): p. 47-58.

12. Noori, J.S., J. Mortensen, and A. Geto, *Recent development on the electrochemical detection of selected pesticides: A focused review*. Sensors, 2020. **20**(8): p. 2221.

13. Anson, F.C., *Innovations in the Study of Adsorbed Reactants by Chronocoulometry*. Analytical chemistry, 1966. **38**(1): p. 54-57.

14. Johnson, D.C. and W.R. LaCourse, *Liquid chromatography with pulsed electrochemical detection at gold and platinum electrodes*. Analytical Chemistry, 1990. **62**(10): p. 589A-597A.

15. Muneer, M. and C. Boxall, *Photocatalyzed degradation of a pesticide derivative glyphosate in aqueous suspensions of titanium dioxide*. International Journal of Photoenergy, 2008. **2008**

16. Cha, S.-K. and Y. Kim, *Deposition of U (VI) at polypyrrole film electrodes modified with chlorophosphon azoIII*. Microchemical journal, 2001. **70**(3): p. 265-273.

17. Sayre, C.N. and D.M. Collard, *Electrooxidative deposition of polypyrrole and polyaniline on self-assembled monolayer modified electrodes*. Langmuir, 1997. **13**(4): p. 714-722.

18. Wang, J., et al., *Electrochemical Study of a Polypyrrole Film/Decanethiol Self-Assembled Monolayer on a Gold Electrode*. Electroanalysis: An International Journal Devoted to Fundamental and Practical Aspects of Electroanalysis, 1999. **11**(18): p. 1345-1349.

19. Lee, J.S., et al., *Disorder–order phase change of ω-(N-pyrrolyl) alkanethiol self-assembled monolayers on gold induced by STM scans and thermal activation*. Physical Chemistry Chemical Physics, 2008. **10**(21): p. 3138-3149.

20. Wang, X., et al., *Specific interaction of platinated DNA and proteins by surface plasmon resonance imaging*. RSC advances, 2016. **6**(26): p. 21900-21906.

21. Ktari, N., et al., *Design of a polypyrrole MIP-SAW sensor for selective detection of flumequine in aqueous media*. Correlation between experimental results and DFT calculations. RSC advances, 2015. **5**(108): p. 88666-88674.